

# Synthesis, Structural and Conductivity studies of Vanadium doped Lithium Lanthanum Titanate for Solid Electrolytes

K. Vijaya Babu\*, V. Veeraiyah, P. S. V. Subba Rao  
Department of Physics, Andhra University, Visakhapatnam - 530 003, A. P., India

Abstract:  $\text{Li}_{0.5-x}\text{La}_{0.5}\text{Ti}_{1-x}\text{V}_x\text{O}_3$  ( $x=0, 0.5, 0.1$  and  $0.15$ ), as solid electrolyte materials, are synthesized by the method of high temperature solid state reaction in air. Their structure and electrochemical performances are characterized by means of X-ray Diffraction, Scanning Electron Microscopy, Raman Spectroscopy, ac-Impedance Spectroscopy and Cyclic Voltammetry. The results of X-ray Diffraction studies reveal that the primitive cells of the materials possess cubic system with perovskite structure corresponds to the  $\text{Pm}\bar{3}\text{m}$  space group ( $Z=1$ ). Also, this structural property is supported by the Raman scattering study. The Scanning Electron Micrographs suggest that the material comprises of polycrystalline microstructure and the grains are distributed homogeneously throughout the surface area. The temperature dependent ionic conductivity investigation of the composite solid electrolyte materials shows the conductivity increase with Vanadium content. Compared to other materials,  $\text{Li}_{0.35}\text{La}_{0.5}\text{Ti}_{0.85}\text{V}_{0.15}\text{O}_3$  material delivers preferably good ionic conductivity. The cyclic voltammetry results indicate that the electrochemical redox reactions takes place in the materials are reversible.

PACS number: 61.10.Nz, 68.37.Hk, 78.30.-j, 66.10.Ed.

Key words: XRD, SEM, Raman spectra, Ionic Conduction.

## 1. INTRODUCTION

Electrolytes are used as ionic conductor inside electrochemical cells. The ionic conductivity inside the cells equals an electronic current flowing in an external circuit between electrodes on opposite sides of the electrolyte. Many ceramic electrolytes have been investigated, although few are evaluated in actual electrochemical cells. The ceramic electrolyte materials include oxides, sulfides, nitrides, halides and a variety of polyanion compositions. Although some impressive lithium conductivities are reported, fabrication and stability issues require further attention [1-3]. The oxide-based ceramic electrolyte, for example, Lithium Lanthanum Titanate,  $\text{Li}_{0.5}\text{La}_{0.5}\text{TiO}_3$ , has high oxidation resistivity with high ionic conductivity [4]. These conductivities are comparable with those of the commonly used liquid electrolyte [5]. However, there are reports that  $\text{La}_{0.56}\text{Li}_{0.33}\text{TiO}_3$  and  $\text{La}_{0.57}\text{Li}_{0.29}\text{TiO}_3$  can intercalate lithium ions in the structure and introduce electronic conductivity at a potential below about 1.7 V vs. Li [6]. In the present work, the structure and the ionic conductivity of LLT samples synthesized with different compositions are compared in order to find an optimum for applications.

## 2. SAMPLE PREPARATION AND EXPERIMENTAL TECHNIQUES

In the process of investigation on the doping effect of vanadium in LLT, the compositions studied are represented by the formula  $\text{Li}_{0.5-x}\text{La}_{0.5}\text{Ti}_{1-x}\text{V}_x\text{O}_3$  ( $x=0, 0.05, 0.1$  and  $0.15$ ) (LLTV). The samples are prepared by Solid State Reaction process. High purity Lithium Oxide (Himedia 99.9%),

Lanthanum (III) Oxide (Himedia 99.9%), Titanium (IV) Oxide (Sigma-Aldrich 99%) and Vanadium (V) Oxide (Himedia 99.9%) powders are used as starting materials.

The stoichiometric mixers of the raw materials are accomplished using agate mortar and pestle. Methanol used as medium is just enough to form slurry to prevent the selective sedimentation of the reagents. The slurry is put on grinding and then heated at  $500^\circ\text{C}$  for 4 hours and calcined at  $800^\circ\text{C}$  for 4 hours in air. Further, the calcined powders are ground in the medium of methanol and recalcined at  $1150^\circ\text{C}$  for 12 hours in air and cooled to room temperature. These synthesized powders are ground again and mixed with polyvinyl alcohol for better compactness among the granules of the material. The powders are pressed at a pressure of 4 ton/Sq.Inch for 10 minutes using hydraulic press into pellets of diameter 10mm and thickness 1 or 2 mm, and finally the pellets are sintered at  $1300^\circ\text{C}$  for 6 hours in air using Muffle Box Furnace.

The phase of the calcined samples are identified by X-ray diffraction with RIGAKU X-ray diffractometer Ultima III (with  $\text{CuK}\alpha$  radiation,  $\lambda=1.5402 \text{ \AA}$ ). The microstructure of the sintered sample is characterized by scanning electron microscopy (SEM) (Carl Zeiss, EVOMA 15, oxford instruments, Inca Penta FET x 3.JPG). Raman experiments are carried out for the calcined sample (Nicolet 6700 FT-Raman spectrometer). The spectrum is recorded from 0 to  $1000 \text{ cm}^{-1}$ . Ionic conductivity for the bulk sample is measured by an AC impedance technique. The surface of the sintered pellet is polished with emery paper, then washed in acetone and dried at  $110^\circ\text{C}$  under vacuum. The

silver paste is pasted both sides of the pellet in order to use as electrodes. The complex impedance is measured using Frequency Response Analyzer in the frequency range 100Hz-1MHz within the temperature range 30 °C to 150 °C. The cyclic voltammetry results are carried out with potential range -1 to 3V at scanning rate 5mV/s using Electrochemical Analyzer (CH instrument, CHI 760C).

### 3. RESULTS AND DISCUSSION

#### 3.1. X-ray Diffraction Analysis

Figure.1 shows the X-ray diffraction patterns of the  $\text{Li}_{0.5-x}\text{La}_{0.5}\text{Ti}_{1-x}\text{V}_x\text{O}_3$  ( $x = 0, 0.05, 0.1$  and  $0.15$ ) materials. This indicated that the primitive cell possesses a cubic system with perovskite structure which corresponds to the  $\text{Pm}\bar{3}\text{m}$  space group ( $Z=1$ ) [7, 8]. The lattice parameter of primitive cell is determined as  $a = 3.8685, 3.8679, 3.8671, 3.8655\text{\AA}$  respectively (figure.2). This value is almost the same as  $a = 3.8734\text{\AA}$  in  $\text{La}_{0.5}\text{Na}_{0.5}\text{TiO}_3$  allowing for the difference of ionic radii [9]. The lattice parameter and the unit cell volume of the LLTV ( $x = 0, 0.05, 0.1$  and  $0.15$ ) decreases with increasing  $x$  values. This is expected as the ionic radius of the  $\text{V}^{5+}$  ( $0.59\text{\AA}$ ) is smaller than that of  $\text{Ti}^{4+}$  ( $0.605\text{\AA}$ ). The density of the samples is found to be around 94% of the theoretical density. The crystallite size of the samples is  $68.51, 75.36, 78.33$  and  $79.79\text{nm}$  calculated by using Scherrer's formula. The variation of the densities (theoretical and experimental), lattice parameter and crystallite size of the compound are shown in table 1.

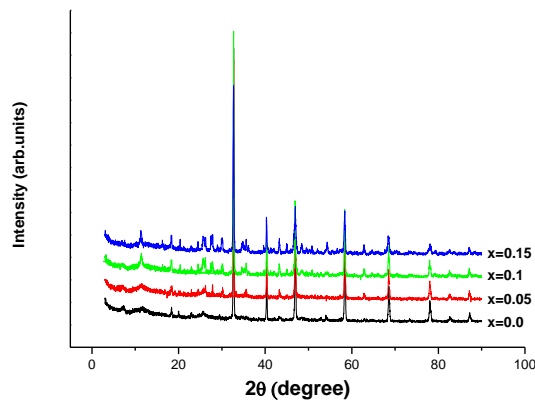


Figure 1: X-ray Diffraction pattern for LLTV ( $x=0, 0.05, 0.1$  and  $0.15$ )

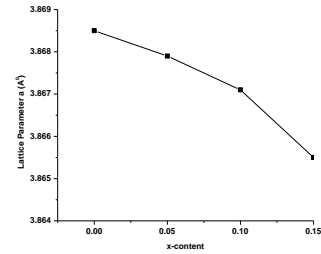


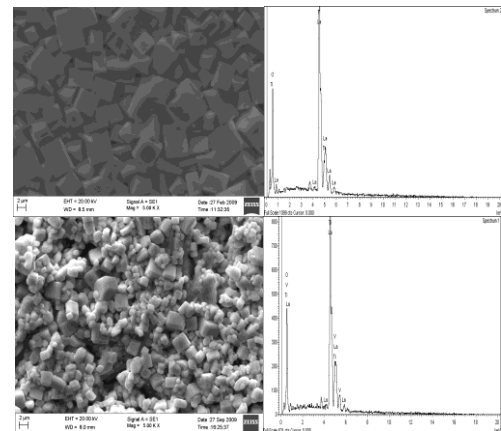
Figure 2: Variation of Lattice Constant with  $x$  value

Table 1: Variation of Densities, Lattice Parameter and Crystallite Size

$x$ -value	Experimental Density ( $\text{g}/\text{cm}^3$ )	Theoretical Density ( $\text{g}/\text{cm}^3$ )	Lattice Parameter ( $\text{\AA}$ )	Crystallite Size (nm)
0	4.8414	4.4600	3.8685	68.51
0.05	4.8381	4.5126	3.8679	75.36
0.1	4.8365	4.5990	3.8671	78.33
0.15	4.8360	4.4246	3.8655	79.79

#### 3.2. SEM and EDS

Figure.3 shows the SEM micrographs, which are taken on the flat smooth surface area of the materials, for LLTV ( $x = 0, 0.05, 0.1$  and  $0.15$ ). The micrographs suggest that the material comprises of polycrystalline microstructure and the grains are distributed homogeneously throughout the surface area. The grain size of the compound is increasing with  $x$ -value, and the average grain size of all samples is calculated by line intercept method to be  $2.2, 1.47, 1.53$  and  $1.66\mu\text{m}$  respectively. The approximate compositions estimated from EDS data agree well with stoichiometric chemical compositions.



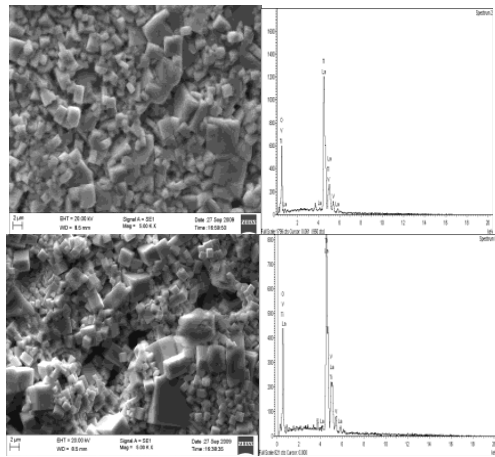


Figure 3: SEM and EDS micrographs of LLTV (x=0, 0.5, 0.1 and 0.15)

### 3.3 Raman Spectra

The Raman spectra of the compound LLTV ( $x = 0, 0.05, 0.1$  and  $0.15$ ) in figure.4 shows five bands which are in good agreement with that of  $\text{La}_{(2-x)/3}\text{Na}_x\text{TiO}_3$  except for the up shift of the bands due to the lighter Li atom compared to Na. Some qualitative trend is observed that all bands are broadened and the intensities are increased with increasing of vanadium content. This may be related to the alleviation of  $\text{TiO}_6$  distortion resulted from the decrease of A-site ordering, which is in good agreement with the XRD results [10]. In cubic phase it has  $O_h$  symmetry and the 15 degrees of freedom divided into twelve optical modes  $3F_{1u}+F_{2u}$ , while another three  $F_{1u}$  symmetry modes correspond to acoustical branch. The 145, 237 and  $528\text{ cm}^{-1}$  comes from the  $F_{1u}$  cubic phase modes [11]. The  $303\text{ cm}^{-1}$  mode come from the splitting of the cubic  $F_{2u}$  mode and the some what broader  $858\text{ cm}^{-1}$  is also resulting in  $F_{1u}$  mode.

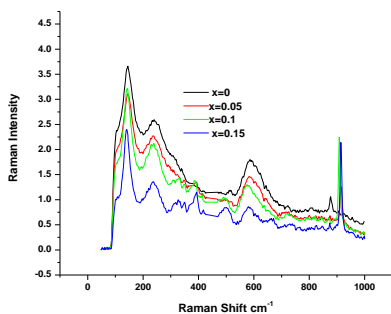


Figure 4: Raman Spectrum of LLTV (x=0, 0.5, 0.1 and 0.15)

### 3.4 Conductivity studies

For instance, at the room temperature the conductivity of  $\text{Li}_{0.5}\text{La}_{0.5}\text{TiO}_3$  is  $1.21 \times 10^{-6}$  S/cm and at higher temperature, its conductivity also increases up to  $1.4 \times 10^{-5}$

S/cm. Comparing with the earlier results obtained by others [12, 13], this is not a good conductivity of Lithium Lanthanum Titanate. Up till now, the bulk and grain boundary conductivity values reported on LLT are subjected to large variations even for the same composition. For example, the bulk conductivity of  $\text{Li}_{1/2}\text{La}_{1/2}\text{TiO}_3$  falls in the range of  $10^{-5} - 10^{-3}$  S/cm at room temperature. This variation indicates that the sample preparation conditions such as sintering temperature may have much influence on the ionic conductivity. We expect this since the volume fractions of grains and grain boundaries in the specimen vary with the grain size, and the grain size normally varies with the sintering temperature and duration. Furthermore, the carrier concentration may also be altered due to possible evaporation of lithium during sintering.

Table 2: Conductivity and Activation Energy for LLTV (x=0, 0.05, 0.1 and 0.15)

x value	AC conductivity at RT (S/cm)	Activation energy (eV)
0	$1.21 \times 10^{-6}$	0.2570
0.05	$4.438 \times 10^{-5}$	0.2954
0.1	$8.546 \times 10^{-5}$	0.2939
0.15	$9.066 \times 10^{-5}$	0.2741

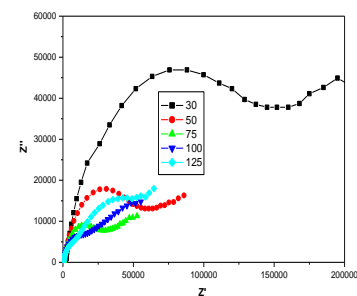


Figure 5: Impedance plots for x = 0

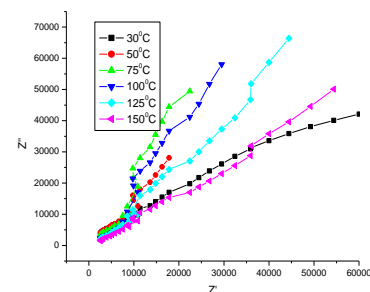


Figure 6: Impedance plots for x = 0.05

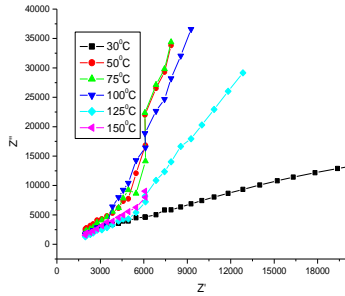


Figure 7: Impedance plots for  $x = 0.1$

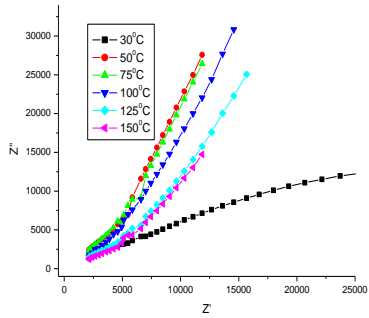


Figure 8: Impedance plots for  $x = 0.15$

Figures 5 to 8 show the typical impedance plot of LLTV ( $x = 0, 0.05, 0.1$  and  $0.15$ ). The semicircular arcs are found to be depressed with their centers lying below the real axis. It is observed that at room temperature all samples show conductivity in the order of  $10^{-5}$  S/cm and as the temperature increases the conductivity also increases. This is due to increase in grain size, which consequently decreases the grain boundary thickness as evidenced by SEM micrographs of these samples. Impedance measurements are carried out for compositions in the range from  $30\text{ }^{\circ}\text{C}$  to  $150\text{ }^{\circ}\text{C}$ . The activation energy of all the samples and the variation of the conductivity with vanadium content are listed in table 2.

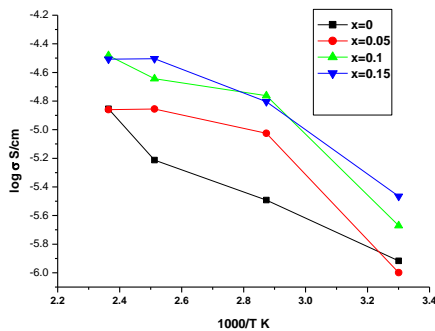


Figure 9: Arrhenius plots for LLTV

The slope of the line will lead us to the activation energy. The Plots between  $\log \sigma$  and  $1000/T$  K are found to be very nearly linear (figure.9). The figure.10 shows the temperature dependence of DC conductivity of LLTV ( $x = 0, 0.05, 0.1$  and  $0.15$ ) which obey the Arrhenius relation.

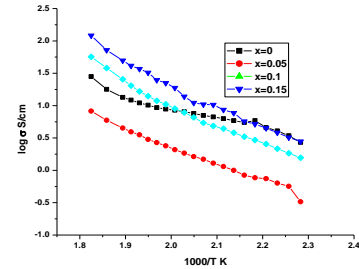


Figure 10: DC Conductivity of LLTV

### 3.5 Cyclic Voltammetry

The LLTV ( $x = 0, 0.05, 0.1$  and  $0.15$ ) solid electrolytes displayed a wide electrochemical stability window are shown by the cyclic voltammetry data. The cyclic voltammograms show broad and poorly resolved cathodic and anodic peak voltages (Figure.11). At  $x=0.05$  it is completely reversible, after that it is going to be poorly reversible. This behavior of the solid electrolytes is probably because of high scan rate ( $5\text{ mV/s}$ ) and structural defects which causes a low mobility for electrical charges either ionic ( $\text{Li}^+$ ) or electronic ( $\text{V}^{n+}$ ). A similar variation of cyclic voltammograms with various partial pressures of oxygen was reported in  $\text{Li}_x\text{Mn}_2\text{O}_4$  thin films [14].

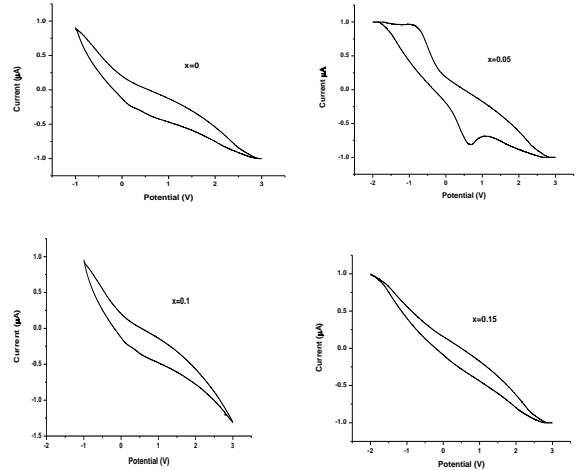


Figure 11: Cyclic Voltammograms of LLTV

We note that non-stoichiometry in the compositions of LLTV samples plays an important role on the electrochemical performance of the micro batteries [15]. The composite exhibits good cycling performance in the

potential range -2.0 to 3.0 V for one cycle. The large anodic current was observed in the potential over 3.0 V and the cycling performance became good, suggesting that this compound can be used as solid electrolyte. These results revealed that  $\text{Li}_{0.5-x}\text{La}_{0.5}\text{Ti}_{1-x}\text{V}_x\text{O}_3$  can be utilized as a solid electrolyte in the all solid state lithium batteries at low potential.

#### 4. CONCLUSIONS

We prepared  $\text{Li}_{0.5-x}\text{La}_{0.5}\text{Ti}_{1-x}\text{V}_x\text{O}_3$  ( $x = 0, 0.05, 0.1$  and  $0.15$ ) compound by solid state reaction method at  $1300^\circ\text{C}$ . By X-ray diffraction measurement of the prepared compound, it is found that the crystal structure is cubic perovskite. The microstructure of the samples is measured by Scanning Electron microscope and the grain size is found to be around  $2\mu\text{m}$ . The bonding nature of the samples is confirmed by Raman spectra. The highest bulk conductivity in the system is  $9.066 \times 10^{-5} \text{ S/cm}$  at RT for the composition corresponding to  $x=0.15$ . The cyclic voltammetry results indicate that the electrochemical reaction is reversible.

#### References:

- [1] Y. Inaguma, L. Chen, M. Itoh, T. Nakamura, T. Ushida, H. Ikuta and M. Wakihara, "High ionic conductivity in lithium lanthanum titanate", *Solid State Comm.*, vol 86, pp 689-693, 1993.
- [2] Y. Inaguma, L. Chen, M. Itoh and T. Nakamura, "Candidate compounds with perovskite structure for high lithium ionic conductivity", *Solid State Ionics*, vol 70/71, pp196-202, 1994.
- [3] Y. Inaguma, J. Yu, Y. J. Shari, M. Itoh and T. Nakamura, A New Charge Storage Mechanism for Electrochemical Capacitors, *J. Electrochem., Soc.* vol 142, pp L6- L8. 1995.
- [4] Yuan Deng, Sui Jun Shang, Ao Mei, Yuan Hua Lin, Li Yu Liu and Ce Wen Nan, "The preparation and conductivity properties of  $\text{Li}_{0.5}\text{La}_{0.5}\text{TiO}_3$ /inactive second phase composites", *J. Alloys and Compounds*. vol 472, pp 456-460, 2009.
- [5] M. Oguni, Y. Inaguma, M. Itoh and T. Nakamura, "Calorimetric and electrical studies on the positional disorder of lithium ions in lithium lanthanum titanate", *Solid State Comm.* vol 91, pp 627-630, 1994.

- [6] Kai Yun Yang, Kuan Zong Fung and Moo Chin Wang, "X-ray photoelectron spectroscopic and secondary ion

mass spectroscopic examinations of metallic-lithium-activated donor doping process on  $\text{La}_{0.56}\text{Li}_{0.33}\text{TiO}_3$  surface at room temperature", *J. Appl. Phys.*, vol 100, pp 056102-056106, 2006.

- [7] He, L. X. and Yoo, H. I., "Effects of B-site ion (M) substitution on the ionic conductivity of  $(\text{Li}_x\text{La}_{2/3-x})_{1+y/2}(\text{M}_y\text{Ti}_{1-y})\text{O}_3$  (M=Al, Cr)", *Electrochimica Acta.*, vol 48, pp 1357-1366, 2003.
- [8] Y. Inaguma, T. Katsumata, M. Itoh, Y. Morii and T. Tsurui, "Structural investigations of migration pathways in lithium ion-conducting  $\text{La}_{2/3-x}\text{Li}_x\text{TiO}_3$  perovskites", *Solid State Ionics.*, vol 177, pp 3037-3044, 2006.
- [9] Bohnke Odile, "The fast lithium-ion conducting oxides  $\text{Li}_x\text{La}_{2/3-x}\text{TiO}_3$  from fundamentals to application", *Solid State Ionics.*, vol 179, pp 9-15, 2008.
- [10] Lazarevic, Z., Romcevic, N., Vijatovic, M, Paunovic, N., Romcevic, M., Stojanovic, B. and Dohcevic Mitrovic, Z., "Characterization of Barium Titanate Ceramic Powders by Raman Spectroscopy", *Acta Physica Polonica A*. vol 115, pp 808-810, 2009.
- [11] Mihailova, B., Bismayer, U., Guttler, B., Gospodinov and M. Konstantinov, L., "Local structure and dynamics in relaxor-ferroelectric  $\text{PbSc}_{1/2}\text{Nb}_{1/2}\text{O}_3$  and  $\text{PbSc}_{1/2}\text{Ta}_{1/2}\text{O}_3$  single crystals", *J. Phys. Condens. Matter.*, vol 14, pp 1091 - 1105, 2002.
- [12] Kim, J. G., Kim, H. G. and Chung, H. T., "Microstructure-Ionic Conductivity Relationships in Perovskite Lithium Lanthanum Titanate", *J. Mater. Sci. Lett.*, vol 18, pp 493-496, 1999.
- [13] Shinichi Furusawa, Hitoshi Tabuchi, Takahiko Sugiyam, Shanwen Tao and John T. S. Irvine, "Ionic conductivity of amorphous lithium lanthanum titanate thin film", *Solid State Ionics.*, vol 176, pp 553-558, 2005.
- [14] C. Julien, E. Haro-Poniatowski, M.A. Camacho-Lopez, L. Escobar-Alarcon, J. Jimenez-Jarquín "Growth of  $\text{LiMn}_2\text{O}_4$  thin films by pulsed-laser deposition and their electrochemical properties in lithium micro batteries" *Materials Science and Engineering B*, vol, 72, pp36-46, 2000.
- [15] Garcia Martin, S., Rojo, J. M., Tsukamoto, H., Moran, E. and Alario-Franco M. A., "Lithium-ion conductivity in the novel  $\text{La}_{1/3-x}\text{Li}_x\text{NbO}_3$  solid solution with perovskite-related structure", *Solid State Ionics*, vol 116, pp 11-18, 1999.